Available online at www.sciencedirect.com
ScienceDirect
Trans. Nonferrous Met. Soc. China 23(2013) 3257−3264
Transactions of Nonferrous Metals Society of China
www.tnmsc.cn

Effect of carbon and boron additions on segregation behavior of directionally solidified nickel-base superalloys with rhenium

Qin HU[1,2], Lin LIU[1], Xin-bao ZHAO[1], Si-feng GAO[1], Jun ZHANG[1], Heng-zhi FU[1]

1. State Key Laboratory of Solidification Processing, Northwestern Polytechnical University, Xi'an 710072, China;
2. Ningbo Branch of China Academy of Ordnance Science, Ningbo 315103, China

Received 22 November 2012; accepted 24 June 2013

Abstract: The phase transformation temperature, segregation behavior of elements and as-cast microstructure were investigated in experimental nickel-base superalloys with different levels of carbon and boron. The results show that the liquidus temperature decreases gradually but the carbide solvus temperature increases obviously with increasing carbon addition. Minor boron addition to the alloy decreases the liquidus temperature, carbide solvus temperature and solidus temperature slightly. Apart from rhenium, the segregation coefficients of the elements alter insignificantly with the addition of carbon. The segregation behavior of rhenium, tungsten and tantalum become more severe with boron addition. The volume fraction and size of primary carbides increase with increasing carbon addition. The main morphology of the carbides is script-like in the alloys with carbon addition while the carbide sheets tend to be concentrated and coarse in the boron-containing alloys.

Key words: carbon; boron; segregation behavior; directional solidification; nickel-base superalloys

1 Introduction

Nickel-base superalloys have been widely used in aircraft and industrial gas turbine. Compared to single-crystal superalloys with the disadvantages such as low yield rate, complex heat treatment process and casting molds, the directionally solidified superalloys have higher yield rate and lower cost.

The minor alloying elements such as boron and carbon were added to the directionally solidified superalloys to strengthen grain boundaries, which led to complex solidification path, partition of elements and precipitated phases in the solidified alloys. Many investigations indicated that the liquidus temperature decreased with the addition of carbon to superalloys, while the rule was different for various alloy systems [1−3]. The addition of carbon would also affect the segregation behavior of elements. AL-JARBA and FUCHS [3] found that the segregation of rhenium would first become severe and then be light with increasing of carbon addition. However, TIN and POLLOCK [4] indicated that carbon addition decreased the segregation degree of rhenium. Moreover, the carbon addition would influence the microstructure such as eutectic and MC type carbides [5−8]. The minor addition of boron to the superalloy would increase boundary interfacial strength, decrease grain boundary diffusivity [9] and modify the morphology of γ' or carbides [9−11]. In addition, the liquidus, carbide solvus and solidus temperature would decrease with the addition of boron [12]. Although there have been many investigations about influence of carbon and boron on segregation characteristics and microstructures of superalloys, the results were different according to the alloys. Studies about effect of carbon and boron on the segregation behavior of elements and microstructures of directionally solidified superalloys especially in the alloys containing rhenium additions were lacking up to now. Moreover, the directionally solidified superalloys containing rhenium have been already used in gas turbine blades. Researches on the role of carbon and boron in segregation and microstructures of these superalloys can provide a valuable basis for the development of the blade materials.

In this work, experimental nickel-base superalloys

Foundation item: Projects (2011CB610406, 2010CB631202) supported by the National Basic Research Program of China; Projects (51101120, 50931004, 51171151) supported by the National Natural Science Foundation of China
Corresponding author: Qin HU; Tel: +86-29-88494080; E-mail: huqin1222@163.com
DOI: 10.1016/S1003-6326(13)62861-7

containing varied contents of carbon and boron were directionally solidified under high thermal gradient. The influences of carbon and boron additions on the phase transformation temperature, segregation behavior of constituent elements and as-cast microstructures were investigated.

2 Experimental

The nominal compositions of the five experimental alloys used in this investigation are listed in Table 1. Cylindrical samples with 4 mm diameter and 70 mm length were directionally solidified in a Bridgeman-type furnace with the coolant of Ga−In−Sn liquid metals. The thermal gradient during processing was about 250 K/cm and a constant withdrawal rate of 50 μm/s was utilized.

The liquidus, carbide solvus and solidus temperatures of the five experimental alloys were investigated by differential scanning calorimeter (DSC) analysis. The prepared samples were heated in an alumina crucible with a heating rate of 10 °C/min. Samples were heated to 1450 °C and then cooled with the same rate to 1100 °C. To avoid the effect of supercooling, only the data during the heating cycle was used.

Standard metallographic techniques were employed for the preparation of samples. To reveal the microstructure, samples were etched with a solution of 3 mL HNO_3+6 mL HF+9 mL $C_3H_8O_3$. The microstructures were analyzed using optical microscopy (OM) and scanning electron microscopy (SEM). The average primary dendrite arm spacing was measured by counting the numbers of dendrites in an optic micrograph with a low magnification in transverse sections. The secondary dendrite arm spacing was estimated in longitudinal sections by counting the numbers of secondary dendrite arm in one length. Quantitative calculation of the phase fraction was performed using the digital image analysis software.

The composition of various constituents and precipitated phase was examined on polished and un-etched samples, using SEM with energy dispersive spectroscopy (EDS) analysis and electron probe micro-analyzer (EMPA) using wavelength dispersive X-ray analysis. Two techniques were used to characterize the solidification segregation behavior of the alloying elements. The specimens were sectioned along the transverse direction at the same position. The first technique was to examine the distribution of elements at discrete locations. At least ten dendritic cores and ten interdendritic regions in transverse section were determined for each sample. The segregation coefficient (k') was then determined by dividing the value of the composition in the dendrite core by the composition in the interdendritic region for each element. The second method was using the point-matrix scanning technique with the EDS analysis. The detailed procedures of the technique can be found in Refs. [13,14]. The representative dendritic structure with a square grid about 300 μm×300 μm of 100 points was scanned. The composition data acquired for individual elements were then ranked according to their characteristic segregation behavior based on the segregation coefficient calculated by the first method.

3 Results

3.1 DSC analysis

The DSC results of the as-cast samples are listed in Table 2. The liquidus temperature and the solidus temperature of baseline alloy are 1397 and 1360 °C, respectively. No carbide solvus is observed in the baseline alloy. The addition of carbon results in a decrease of liquidus first and an increase of carbide

Table 1 Composition of experimental alloys (mass fraction, %)

Alloy	Cr	Co	Mo	W	Ta	Al	Hf	Re	C	B	Ni
1	4.96	12.1	1.02	5.81	8.03	6.08	0.05	5.05	−	−	Bal.
2	5.04	11.9	1.00	6.02	8.19	5.98	0.09	5.11	0.040	−	Bal.
3	5.05	12.0	1.03	6.00	8.14	5.99	009	5.08	0.085	−	Bal.
4	5.07	12.0	1.02	6.03	8.10	5.96	0.09	5.13	0.045	0.014	Bal.
5	5.04	12.0	1.01	6.03	8.18	6.05	0.08	5.18	0.085	0.010	Bal.

Table 2 DSC results of as-cast samples

Alloy	Liquidus temperature/°C	Carbide solvus temperature/°C	Solidus temperature/°C	Freezing range/°C
1	1397	−	1360	37
2	1391	1370	1351	40
3	1388	1377	1353	35
4	1389	1364	1348	41
5	1386	1371	1350	36

solvus temperature. The solidus temperature is observed to decrease but then increase slightly with the addition of carbon. As shown in Table 2, the boron addition makes the liquidus temperature, carbide solvus temperature and solidus temperature all decreased slightly. It also can be seen that the freezing range does not alter significantly with the addition of carbon and boron.

3.2 Microstructure

The backscattered SEM images of the five experimental alloys on transverse section (Fig. 1) show a typical dendritic microstructure of a directionally solidified nickel-base superalloy. For alloys with carbon addition, plenty of carbides precipitate in the interdendritic region. With higher carbon addition, carbides are interconnected networks of carbide sheets and occupy the most area of the interdendritic region especially when the carbon content is high. The volume fraction and size of the carbides increase obviously with the increasing of carbon content, but the relatively high carbon addition does not cause change in the carbide morphology. The main morphology of the carbides is also script-like when boron is added to the alloys. It can be seen from Table 3 that the change of volume fraction of the carbides is very little when 0.014% (mass fraction) boron is added to Alloy 2. However, the comparison of Alloy 3 and Alloy 5 shows that the volume fraction of carbides decreases with boron addition. Moreover, the measuring results of the dendrite arm spacing can be seen from Table 3 which clearly shows that the additions of carbon and boron do not significantly alter the primary and secondary dendrite arm spacing.

3.3 Segregation behavior of elements

Figures 2 and 3 show the result of the calculated segregation coefficient (k') which was measured using the discrete point measurement technique. It can be found that elements such as rhenium, tungsten and cobalt segregate to the dendrite core. Elements such as tantalum, molybdenum and aluminum segregate to the interdendritic region. The segregation coefficient of nickel and chromium is close to unity. It can also be seen

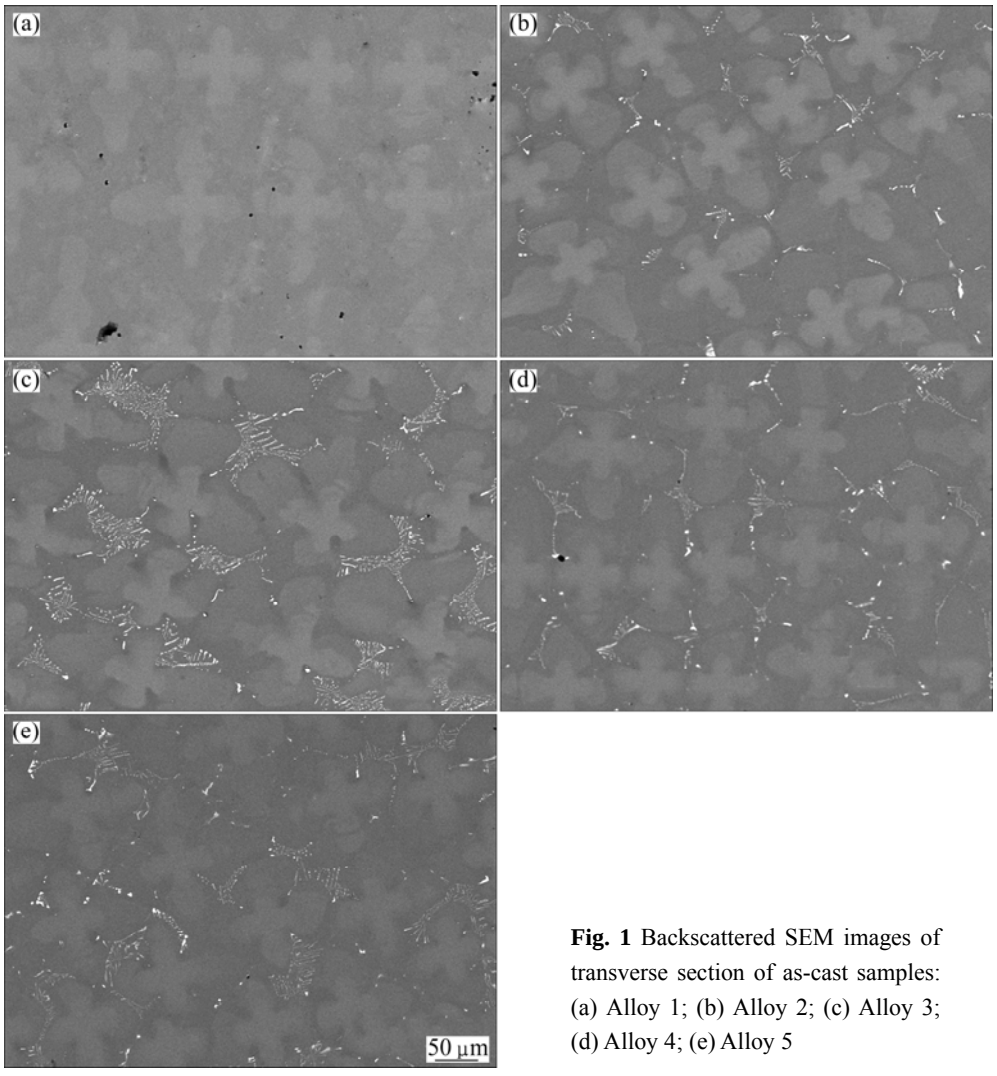

Fig. 1 Backscattered SEM images of transverse section of as-cast samples: (a) Alloy 1; (b) Alloy 2; (c) Alloy 3; (d) Alloy 4; (e) Alloy 5

Table 3 Primary and secondary dendrite arm spacing and volume fraction of carbides

Alloy	λ_1/μm	λ_2/μm	Carbide volume fraction/%
1	167.7	38.4	0
2	169.6	35.7	3.1
3	164.0	37.2	7.9
4	156.2	33.5	3.5
5	151.7	32.2	6.9

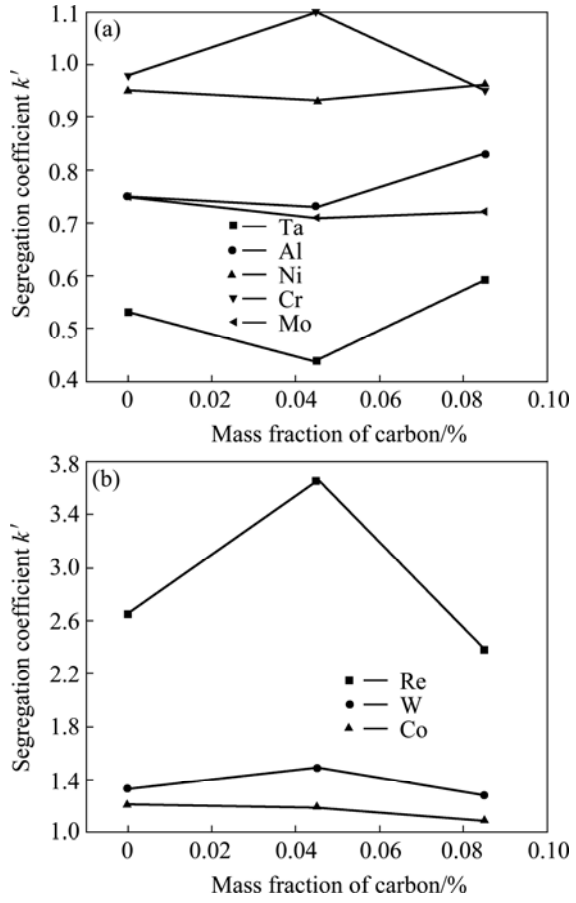

Fig. 2 Segregation coefficients of different elements with varying carbon content: (a) Elements segregating to interdendritic; (b) Elements segregating to dendrite core

that Re, W, Ta and Al segregate more strongly with the addition of 0.04% carbon and then the segregation degree decreases when the content of carbon reaches to 0.085%. In general, apart from Re, the segregation coefficient of the elements does not alter significantly with the increasing addition of carbon to the alloy. This result is similar to the study of AL-JARBA and FUCHS [3], but different from that of TIN and POLLOCK [4]. Figure 3 indicates that the addition of boron leads to severe segregation for Re, W and Ta and has no obvious influence on other elements. Similar to the result of carbon addition, the segregation coefficient of the elements does not change obviously with boron addition except for Re.

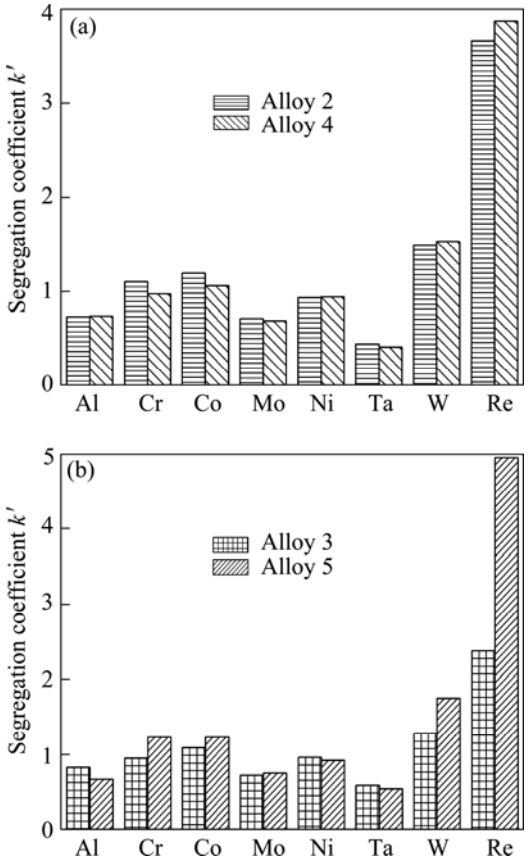

Fig. 3 Effect of boron addition on segregation coefficients of different elements: (a) Comparison in Alloy 2 and Alloy 4; (b) Comparison in Alloy 3 and Alloy 5

The results of the point-matrix scanning technique are shown in Fig. 4. It indicates that the segregation degree of Re and Ta firstly increases and then decreases with the addition of carbon to the alloy. Considering the back diffusion, BRODY and FLEMINGS obtained the equation known as the B-F model which can be written as

$$c_s = kc_0[1-(1-2\alpha k)f_s]^{\frac{k-1}{1-2\alpha k}} \quad (1)$$

where C_s is the composition of the solid; k is the distribution coefficient; C_0 is the initial composition of the liquid; f_s is the fraction solid; α is the solutal Fourier number. Then distribution coefficients were determined by fitting the B-F model to the experimental data. In all cases, a Fourier number of 0.01 is used to account for the limited back diffusion during solidification. Comparison of the experimental data and fitted B-F model for Re and W in Alloy 2 is shown in Fig. 5 which show good agreement except in the early stages and final stages of solidification. Good agreement could be found for all other constituent elements. Assessments of the distribution coefficients for constituent elements in experimental alloys are listed in Table 4 which clearly

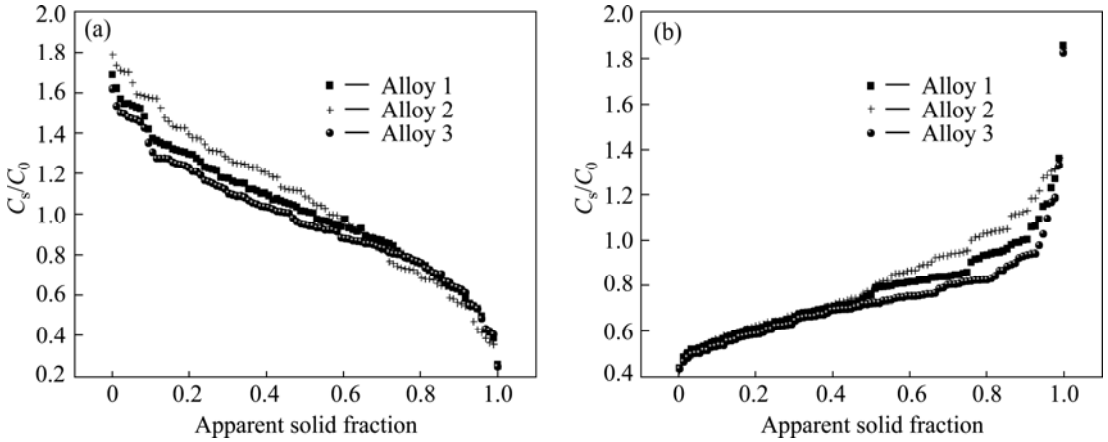

Fig. 4 Effect of carbon additions on segregation behavior of elements: (a) Re; (b) Ta

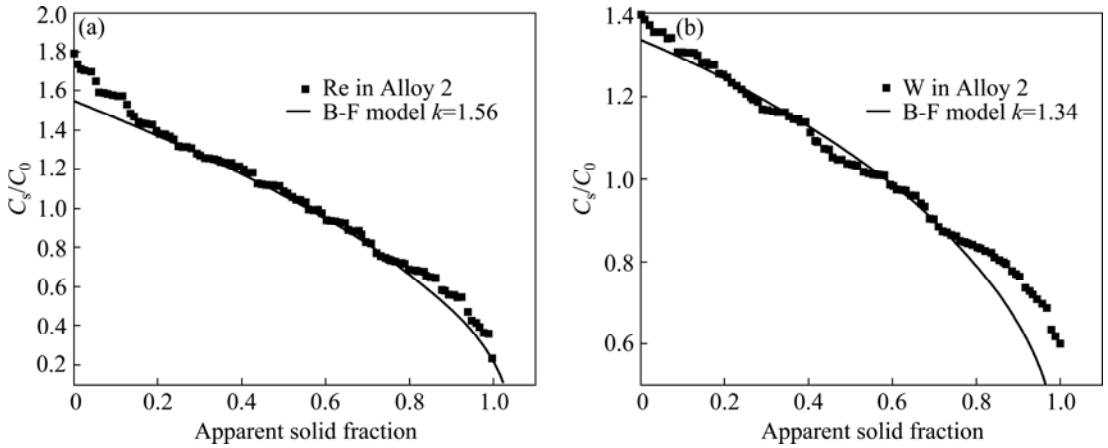

Fig. 5 Comparison of experimental data of Re (a) and W (b) in Alloy 2 with fitted B-F model

Table 4 Fitted distribution coefficients for constituent elements in experimental alloys

Alloy	Distribution coefficient							
	Cr	Co	Mo	Al	Ta	Re	W	Ni
1	0.99	1.09	0.81	0.80	0.61	1.39	1.27	0.97
2	1.02	1.07	0.78	0.81	0.58	1.56	1.34	0.96
3	0.98	1.07	0.79	0.83	0.65	1.36	1.24	0.96
4	0.99	1.06	0.79	0.80	0.59	1.59	1.36	0.95
5	1.01	1.08	0.81	0.78	0.62	1.45	1.29	0.94

show that the effect of carbon and boron addition to the segregation of Re is greater than that of other constituent elements.

4 Discussion

4.1 Effect of carbon and boron on microsegregation

It has been obtained that the segregation behavior of rhenium is significantly affected by increasing the carbon addition. Rhenium is one of the main strengthening elements in nickel-base superalloys with high content of refractory elements. Rhenium retards the diffusion controlled γ' coarsening and significantly improves the high-temperature creep properties [15−17]. However, the Re addition also leads to a series of problems such as the formation of TCP phase and grain defect [18]. Therefore it is necessary to analyse the segregation behavior of rhenium.

As mentioned before, the addition of carbon and boron does not significantly alter the freezing range and primary and secondary dendrite arm spacing. Moreover, the withdrawal rate utilized in this work is constant. Therefore, the thermal solutal convection may act as the major factor affecting the segregation of solution

elements. For similar Ni-base alloys used in this work, numerical investigation concludes that the liquid density changes by compositional differences are much greater than that by thermal gradients. During the directional solidification, the segregation of solution elements, such as Re and W which segregate to the dendrite core, and elements such as Al which are rejected to the interdendritic region, makes the interdendritic liquid have an average density lower than that of the liquid above it. This density difference caused by the segregation of solute elements results in the lower density liquid at the bottom of the interdendritic region flowing up to the top of the mushy zone which may contribute to the homogenization of solution elements. The content of rhenium and tungsten is high in the alloys used in this work, which results in larger density inversion and buoyancy force driving convection flow. However the high concentration of tantalum in the alloys which segregates to the interdendritic region would offset the density difference and suppress the thermal solutal convection due to the high density of tantalum. Meanwhile, the addition of carbon to the alloy results in the formation of carbides precipitated in the interdendritic region. The role of the carbides is bifacial to the thermal solutal convection. On the one hand, the precipitation of Ta-rich carbides aggravates density inversion since it would delete tantalum in the liquid. On the other hand, the precipitation and coalescence of carbides in the interdendritic region lowers the permeability of the dendritic network and retards the local fluid flow. The effect of the thermal solutal convection on the microsegregation depends on the solid fraction.

The onset of fluid flow due to the thermal solutal convection works when the fraction of solid is low. The computer simulation of nickel-base superalloy [19] showed that a temperature of 11°C below the liquidus temperature of the alloy would typically correspond to a solid fraction of about 30%. It can be found in Table 2 that the carbide solvus temperature is measured to be 21 °C below the liquidus temperature in Alloy 2. The solid fraction would be so high that the onset of thermal solutal convection is confined within the mushy zone and the precipitation of carbide networks lowers the permeability of the interdendritic region which suppresses the thermal solutal convection further. So the segregation degree of rhenium in Alloy 2 is greater than that in Alloy 1. The carbide solvus temperature in Alloy 3 is measured to be 11 °C which is below the liquidus temperature. The solid fraction is still small when the carbides appear. Meanwhile, the precipitation of Ta-rich carbides aggravates density inversion. Therefore, stronger thermal solutal convection would make the segregation of rhenium decreased in Alloy 3 compared to that in Alloy 2.

It can be seen from Table 2 that the range between the liquidus temperature and the carbide solvus temperature in Alloy 2 is 21 °C and that in Alloy 4 is 25 °C. The effect of only 4 °C difference to the segregation of elements can be neglected in the case of high solid fraction. The comparison of the carbide precipitates in Alloy 2 and Alloy 4 shows that the carbide morphology and fraction are almost the same in both alloys. Therefore, the influence of the minor addition of boron to Alloy 2 on the segregation behavior of elements is quite confined. The situation is extremely different when minor boron is added to Alloy 3. The range between the liquidus temperature and the carbide solvus temperature in alloy 3 is 11 °C and that in alloy 5 is 15 °C. If a temperature of 11 °C below the liquidus temperature corresponds to a solid fraction of 30%, with a freezing range of approximately 40 °C, a temperature of 15 °C below the liquidus temperature would correspond to a solid fraction of about 40% if a linear relationship exists between fraction solid and the freezing range of the alloy. Unfortunately, the relationship is not typically linear during dendrite solidification and the solid fraction would be more than 40% correspond to a temperature of 15 °C below the liquidus temperature in practice. So when the carbides precipitate at a temperature of 15 °C below the liquidus temperature, the solid fraction is large enough to restrain the thermal solutal convection. Although the size and fraction of carbides in Alloy 5 are smaller compared to those in Alloy 3, which decrease the impact of carbide networks, the influence of thermal solutal convection in Alloy 3 is stronger than that in Alloy 5, which is the key factor determining the segregation behavior of elements. Therefore, rhenium segregates more strongly in Alloy 5 than in Alloy 3.

4.2 Carbides

The addition of carbon to the baseline alloy results in the formation of carbide precipitates precipitate in the interdendritic region. The concentrations of elements of the script-like carbides in Alloy 2 and Alloy 4 are listed in Table 5. It indicates the incorporation of boron into the MC carbides in nickel-based superalloys which has also been observed in previous work [10], but the addition of boron dose not significantly affect the other component elements of carbides. It can be found from Fig. 6 that the carbide sheets of boron-containing alloys were more concentrated and coarse than that of none boron-containing alloys. In turn, this may be used for explaining the incorporation of boron into the MC carbides in boron-containing alloys. In the boron containing alloy, carbon atoms may be replaced by the boron atoms during the formation of carbides. The large atom size of boron makes the misfit of MC/γ higher. It is

Table 5 Concentration of elements of carbide in Alloy 2 and 4

Alloy	Cr	Co	Mo	W	Ta	Al	Hf	Ni	C	B
2	1.5	1.4	1.9	6.3	64.9	0.9	1.6	9.2	12.5	0
4	1.7	1.5	1.8	6.1	65.7	0.7	1.4	8.9	10.4	1.6

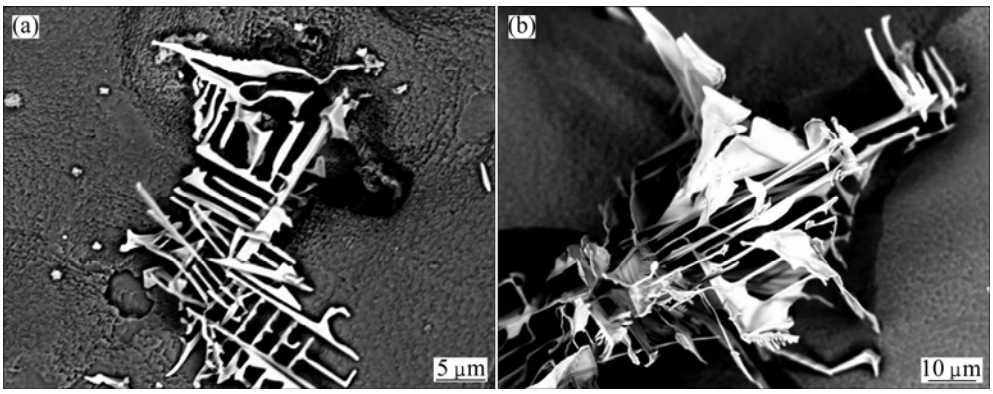

Fig. 6 Morphologies of script carbides revealed by deep etching: (a) Alloy 2; (b) Alloy 4

no doubt that large misfit energy intends to reduce the surface area of the precipitate. So the carbide sheets tend to be bulk in the boron-containing alloys.

5 Conclusions

1) The liquidus temperature decreases gradually and the carbide solvus temperature increases obviously with increasing of carbon additions. Minor boron addition to the alloy makes the liquidus temperature, carbide solvus temperature and solidus temperature all decreased slightly. The freezing range also changes inconsiderably with the addition of carbon and boron.

2) The segregation coefficient of the constituent elements is measured by the EDS analysis. It shows that the segregation coefficient of rhenium first increases and then decreases with the increasing of carbon addition, while the segregation behavior of other elements does not alter significantly with the addition of carbon. The elements of Re, W and Ta segregate more strongly with the minor boron addition to the alloy.

3) The carbides are predominantly script-like morphology in all the carbon containing alloys. The volume fraction and the size of carbides increase obviously with the increasing of carbon content, but the relatively high carbon addition does not cause obvious change in the carbide morphology. The primary and secondary dendrite arm spacing are not greatly influenced by the carbon and boron additions.

References

[1] WASSON A J, FUCHS G E. Microstructural evolution of a carbon modified single crystal Ni-base superalloy [J]. Materials Characterization, 2012, 74: 11−16.

[2] YU Z H, LIU L, ZHAO X B, ZHANG W G, ZHANG J, FU H Z. Effect of solidification rate on MC carbide morphology in single crystal Ni-base superalloy AM3 [J]. Transactions of Nonferrous Metals Society of China, 2010, 20(10): 1835−1840.

[3] AL-JARBA K A, FUCHS G E. Effect of carbon additions on the as-cast microstructure and defect formation of a single crystal Ni-based superalloy [J]. Materials Science and Engineering A, 2004, 373: 255−267.

[4] TIN S, POLLOCK T M. Phase instabilities and carbon additions in single-crystal nickel-base superalloys [J]. Materials Science and Engineering A, 2003, 348: 111−121.

[5] ZHOU Y Z, VOLEK A. Effect of carbon additions on hot tearing of a second generation nickel-base superalloy [J]. Materials Science and Engineering A, 2008, 479: 324−332.

[6] MIAO Z J, SHAN A D, WU Y B, LU J, HU Y, LIU J L, SONG H W. Effect of P and B addition on as-cast microstructure and homogenization parameter of Inconel 718 alloy [J]. Transactions of Nonferrous Metals Society of China, 2012, 22(2): 318−323.

[7] WEI C N, BOR H Y, CHANG L. The influence of carbon addition on carbide characteristics and mechanical properties of CM-681LC superalloy using fine-grain process [J]. Journal of Alloys and Compounds, 2011, 509: 5708−5714.

[8] WEI C N, BOR H Y, CHANG L. The effect of carbon content on the microstructure and elevated temperature tensile strength of a nickel-base superalloy [J]. Materials Science and Engineering A, 2010, 527: 3741−3747.

[9] GAROSSHEN T J, TILLMAN T D, MCCARTHY G P. Effect of B, C, and Zr on the structure and properties of a P/M nickel base superalloy [J]. Metallurgical and Materials Transactions A, 1987, 18(A): 69−77.

[10] YAN B C, ZHANG J, LOU L H. Effect of boron additions on the microstructure and transverse properties of a directionally solidified superalloy [J]. Materials Science and Engineering A, 2008, 474: 39−47.

[11] SHULGA A V. Boron and carbon behavior in the cast Ni-base superalloy EP962 [J]. Journal of Alloys and Compounds, 2007, 436: 155−160.

[12] CUTLER E R, WASSON A J, FUCHS G E. Effect of minor alloying additions on the carbide morphology in a single crystal Ni-base superalloy [J]. Scripta Materialia, 2008, 58: 146−149.

[13] HOBBS R A, TIN S, RAE C M F. A castability model based on

elemental solid-liquid partitioning in advanced nickel-base single-crystal superalloys [J]. Metallurgical and Materials Transactions A, 2005, 36: 2761−2773.

[14] GANESAN M, DYE D, LEE P D. A technique for characterizing microsegregation in multicomponent alloys and its application to single-crystal superalloy castings [J]. Metallurgical and Materials Transactions A, 2005, 36: 2191−2204.

[15] CHENG Y, ZHANG H, SONG L W, MA Y, LI S S, GONG S K. Effect of Re element on oxidation resistance of Ni_3Al−Mo based alloys at 1150 degrees C [J]. Transactions of Nonferrous Metals Society of China, 2012, 22(2): 510−515.

[16] RUSING J, WANDERKA N, CZUBAYKO U, NAUNDORF V, MUKHERJI D, ROSLER J. Rhenium distribution in the matrix and near the particle-matrix interface in a model Ni−Al−Ta−Re superalloy [J]. Scripta Materialia, 2002, 46: 235−240.

[17] GUAN X R, LIU E Z, ZHENG Z, YU Y S, TONG J, ZHAI Y C. Solidification behavior and segregation of Re-containing cast Ni-base superalloy with different Cr content [J]. Journal of Materials Science and Technology, 2011, 27(2): 113−117.

[18] RAE C M F, REED R C. The precipitation of topologically close-packed phase in rhenium-containing superalloys [J]. Acta Materialia, 2001, 49: 4113−4125.

[19] BECKERMANN C, GU J P, BOETTINGER W J. Development of a freckle predictor via rayleigh-number method for single-crystal nickel-based superalloy castings [J]. Metallurgical and Materials Transactions A, 2000, 31: 2545−2557.

碳和硼对高铼含量的定向凝固镍基高温合金元素偏析行为的影响

胡 勤[1,2]，刘 林[1]，赵新宝[1]，高斯峰[1]，张 军[1]，傅恒志[1]

1. 西北工业大学 凝固技术国家重点实验室，西安 710072；
2. 中国兵器科学研究院宁波分院，宁波 315103

摘 要：研究元素碳和硼对含铼镍基定向柱晶高温合金相转变温度、元素偏析和碳化物析出相的影响。结果表明：随着碳含量的增加，液相线温度逐步降低，而碳化物的析出温度上升。硼的添加造成合金液相线温度、碳化物析出温度和固相线温度均下降。随着碳含量的增加，铼元素的偏析先增大后减小，而其它元素的偏析程度变化并不是很大。铼、钨、钽的偏析随硼的加入而逐渐增大。合金中碳化物的形态主要为汉字体状，碳化物数量随着碳含量的增加逐渐增大。添加硼元素的合金中析出的碳化物较不含硼元素的合金中析出的碳化物更加集中和粗大。

关键词：碳；硼；偏析行为；定向凝固；镍基高温合金

(Edited by Chao WANG)